NON-LINEAR SPECTRUM SENSING SCHEME IN IMPULSIVE NOISE ENVIRONMENTS FOR COGNITIVE RADIO

Dr. Walid K. Ghamry

Assistant Professor, Department of Computer Engineering,

Al-Baha University, Saudi Arabia

wkamal@bu.edu.sa

Abstract : Recently, prior studies have addressed and solved the issues of spectrum sensing through Cognitive Radio (CR) technology, assuming that the noise is Gaussian. However, in real-world scenarios, this assumption often falls short as various types of noise exhibit non-Gaussian and impulsive characteristics. Consequently, there is significant value in investigating spectrum sensing techniques that are specifically tailored to operate effectively in impulsive noise presence. Hence, within the context of CR networks operating in impulsive noise environments, multiple reception antennas are used to tackle the challenge of spectrum sensing. To efficiently deal with the unique characteristics of impulsive noise, which manifest as a heavy-tailed probability density function, an innovative non-linear combining scheme is introduced, founded on the arranging statistics. The simulation results confirm that the introduced scheme consistently offers robust performance and stability in spectrum sensing and outperforms conventional methods in terms of detection performance, up to 65%, within impulsive noise environments.

Keywords: Spectrum sensing, impulsive noise, cognitive radio, multiple antenna, GLRT

1. Introduction

The hasty proliferation of wireless communication services and devices in recent years has led to an increased demand for spectrum resources. A promising solution for this spectrum paucity issue has emerged in cognitive radio technology [1, 2]. The concept behind cognitive radio (CR) involves conducting spectrum sensing, detecting unoccupied spectrum holes currently unutilized by primary users (PUs), and subsequently employing these available spectrum holes without interfering with PUs [3]. To detect and identify underutilized or unoccupied frequency bands, a variety of spectrum sensing approaches have been put forward in academic literature. These include energy detection sensing [4], cyclostationary-based sensing [5], eigenvalue-based sensing [6], and matched filtering [7]. A Gaussian noise distribution is often assumed in the majority of spectrum sensing schemes. While this assumption is generally reasonable, communication systems can often encounter impulsive noise environments [8].

An impulsive noise model can accurately describe the noisy conditions within a CR, particularly when influenced by factors like lightning in the atmosphere, moving vehicles, car ignition, and nearby motors. Many efforts at cognitive radio networks have focused on addressing spectrum sensing challenges operating within non-Gaussian noise environments. In [9], an innovative cyclic correlation estimator is introduced, relying on the utilization of multivariable sign function. The present study specifically investigates the symmetric α-stable distribution, indicated as SαS, along with both of its particular instances, namely the Gaussian and the Cauchy

distributions. The work in [10] proposes a Combining with Order Statistics (COS) technique for spectrum sensing in cognitive radios incorporating receive diversity. The study leverages a nonlinear diversity-combining approach in environments characterized by contaminated Gaussian, Cauchy, Gaussian noise distributions.

In [11], an energy detection based method is introduced to tackle the performance decline associated with energy detection under variance noise environments. In [12], the authors specifically focus on tackling the problem of spectrum sensing within a non-Gaussian noise environment. They propose the utilization of a novel statistical measure function known as "circular correntropy" to tackle this specific issue. The work in [13] introduces an innovative Kendall's tau (KT) based detection method designed to identify primary signals in the presence of additive non-Gaussian noise, specifically described by the contaminated Gaussian model (CGM). A p-norm detector is designed for spectrum sensing in [14] to account for the heavy-tailed characteristics of noise encountered in practical scenarios by modelling the channel noise through a generalized Gaussian distribution. The work in [15] presents a novel spectrum sensing method designed to ascertain the signal's presence amid impulsive noise using only sampled data. The proposed algorithm constructs the test statistic employing the similarity measure of samples and maximizes the system reliability with fewer samples.

In this paper, a non-linear spectrum sensing scheme is proposed for CR networks featuring multiple receive antenna branches, specifically designed to operate effectively in impulsive noise environments. This scheme is referred to as "arranging and picking of observations (APO)". The APO scheme harnesses non-linear combining strategies in conjunction with the Generalized Likelihood Ratio Test (GLRT) detector to effectively handle the characteristics of heavy-tailed probability density function associated with impulsive noise. This non-linear approach relies on arranging statistics to achieve its objectives. To be more specific, the GLRT detector generates the log-likelihood ratios (LLRs) that are used as the test statistic in the APO scheme. These LLRs are computed by carefully selecting set of observations with low magnitudes, chosen from the collective observations obtained from the various branches of a receiver (receive antennas).

This paper's contributions can be summed up in two key aspects:
- The paper introduces an innovative spectrum sensing scheme designed explicitly for cognitive radio networks featuring receiver diversity.
- The paper conducts a performance comparison across diverse noise environments between the proposed APO scheme and conventional schemes. This comparative analysis provides valuable insights into the scheme's effectiveness and robustness in practical scenarios.

This paper is structured as follows: Section two introduces the impulsive noise and system model for the proposed APO scheme, while Section three offers an in-depth description of the APO scheme. Section four conducts the performance evaluation of APO scheme. Section five concludes the research study.

2. System and Impulsive Noise Model

2.1. System Model

Within the CR system model, an observed signal can be acquired either by simultaneously collecting data from multiple antennas at a single time instant or via consolidating data from a single antenna across multiple

consecutive time instants. Suppose a CR is fitted out with M receiving antennas and a PU with a single transmit antenna. It is assumed that each of the CR's antennas collects N samples, representing the sample size within an observation period. The observed signal at the nth time instant on the mth receive antenna branch is provided by

$$y_m(n) = g_m(n)\ s(n) + w_m(n), \qquad (1)$$

where $y_m(n) = y_{m,I}(n) + j\ y_{m,Q}(n)$ denotes the low-pass discrete-time observation with the subscripts Q and I signify the quadrature and in-phase components, respectively, and $s(n) = s_I(n) + j\ s_Q(n)$ represents the PU's transmitted signal. In addition, the complex gain coefficients of the channel existing between mth receive antenna branch and PU are represented as $g_m(n) = g_{m,I}(n) + j\ g_{m,Q}(n)$, and $w_m(n) = w_{m,I}(n) + j\ w_{m,Q}(n)$ represents identically and independent distributed ($i.i.d$) complex additive noise components characterized by a shared joint probability density function fw_I, w_Q of $\{(w_{m,I}(n), w_{m,Q}(n))\}$. Two hypotheses exist, namely:

$$\begin{cases} H_0 : y_m(n) = w_m(n) \\ H_1 : y_m(n) = g_m(n)\ s(n) + w_m(n), \end{cases} \qquad (2)$$

where H_0 corresponds to the null hypothesis, signifying that a primary user signal is absent, and H_1 indicates that a primary user signal is present. In this context, the decision rule (test statistic) can be represented as

$$TS(Y) \underset{H_0}{\overset{H_1}{\gtrless}} \tau, \qquad (3)$$

where $TS(Y)$ represents a function of the observation signal $N \ x \ M$ matrix $Y = [\bar{y}_1, \bar{y}_2, \cdots, \bar{y}_m]$, with $\bar{y}_m = [y_1(n), y_2(n), \cdots, y_m(N)]^T$ represents $N \ x \ 1$ observation vector at mth receive antenna branch, and τ is the threshold to be determined that satisfies the constraint $\Pr\{TS(Y) > \tau \mid H_0\}$ on false alarm probability.

2.2. Impulsive Noise Model

In this system model, the complex Stable α-Stable (SαS) noise model is adopted [16], specifically utilizing the bivariate isotropic Stable α-Stable (BISαS) probability density function (PDF) as the common joint PDF fw_I, w_Q.

$$fw_I, w_Q(u,v) = \frac{1}{(2\pi)^2} \int_{-\infty}^{\infty} \int_{-\infty}^{\infty} \exp\{ -\gamma(t^2 + z^2)^{\frac{\alpha}{2}}$$
$$- j(tu + zv)\}\ dtdz, \quad -\infty < u,\ v < \infty \qquad (4)$$

In (4), the positive dispersion parameter γ is linked to the extent of spread in the SISαS PDF, while the characteristic exponent α, falling within the range (0, 2), and characterizes the heaviness of the tails in the SISαS PDF. The PDF (4) does not have an available closed-form expression, except for specific cases such as α=1 and α=2. Specifically, when α=1, the PDF (4) corresponds to the bivariate Cauchy PDF

$$f_{W_I}, W_Q (u, v) = \frac{1}{2\pi(u^2 + v^2 + \gamma^2)^{\frac{3}{2}}} \quad -\infty < u, \ v < \infty \tag{5}$$

Furthermore, when α=2, the PDF (4) transforms into the bivariate Gaussian PDF

$$f_{W_I}, W_Q (u, v) = \frac{1}{2\pi\sigma^2} e^{-\frac{u^2+v^2}{2\sigma^2}} , \quad -\infty < u, \ v < \infty , \tag{6}$$

with $\sigma^2 = 2\gamma$, representing the noise variance. This also aligns with the limit where there is no impulsiveness in the distribution.

3. The APO Spectrum Sensing Scheme

The spectrum sensing scheme is divided into two stages: 1) arranging and picking of specific observations, and 2) log-likelihood ratios (LLRs) test statistic.

3.1. Arranging and Picking of Specific Observations

In environments characterized by impulsive noise, non-linear schemes across various applications of signal processing have proven effective in reducing the impact of noise components [17]. In such impulsive noise scenarios, it is often the case that observations with larger magnitudes are more likely to be influenced by noise components as opposed to signal components. Therefore, a favorable approach for enhancing performance is to select observations having smaller magnitudes, which can be achieved through non-linear schemes based on arranging statistics. This approach helps improve the robustness of signal detection when dealing with impulsive noise. Inspired from the aforementioned concepts and illustrated in Fig. 1, the APO scheme receives the observed N samples from each mth receive antenna branch and collects them in an observation signal $N \ x \ M$ matrix Y as outlined below:

$$Y = \begin{bmatrix} Y_{11} & Y_{12} & \cdots & Y_{1M} \\ Y_{21} & Y_{22} & \cdots & Y_{2M} \\ \vdots & \vdots & \ddots & \vdots \\ Y_{N1} & Y_{N2} & \cdots & Y_{NM} \end{bmatrix} \tag{7}$$

Then the observation signal matrix Y is transformed to one row vector of size $1 \ x \ NM$ utilizing Vectorization. The columns of the matrix Y are appended (in order) to form the vector $\bar{x}$ as outlined below:

$$\bar{x} = \text{vec}\ (Y) = \{Y_{11}, Y_{21}, \cdots, Y_{N1}, Y_{12}, Y_{22}, \cdots, Y_{N2}, \cdots, Y_{NM}\}$$

(8)
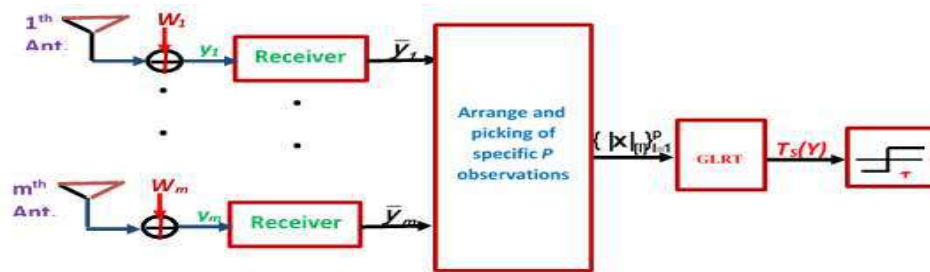
Fig. 1 The APO spectrum sensing scheme

Consequently, arranging the absolute values of the complex vector $\bar{x}$ elements in ascending order yields the following magnitude ranking statistic absolute values vector:

$$|x|_{[\cdot]} = \{|x|_{[1]}, |x|_{[2]}, \cdots, |x|_{[NM]}\}$$

(9)

In this context, $|x|_{[I]}$ represents the ith smallest observations from the NM absolute values present in $\bar{x}$ and is referred to the ith magnitude ranking statistic.

This implies that $|x|_{[1]} \leq |x|_{[2]} \leq \cdots \leq |x|_{[NM]}$

(10)

Subsequently, a specific set $\{|x|_{[1]}, |x|_{[2]}, \cdots, |x|_{[P]}\}$ consisting of the P smallest ranking absolute values observations is picked and sent to the $GLRT$ detector to generate the test statistics as illustrated in Fig. 1, where $1 \leq P \leq NM$.

3.2. Log-likelihood ratios (LLRs) test statistic

In the second stage of the APO scheme, the test statistic is derived from the LLRs generated by the GLRT detector, as depicted in Fig. 1. In scenarios where the cognitive radio lacks information about the noise variance, characteristics such as pilot patterns, modulation schemes of the primary user signal, as well as the channel gain between the CR and PU, Maximum Likelihood Estimates (MLEs) are often used in this situation to replace the unknown parameters. Consequently, the assumption is made that the noise power is known, and PU faded complex transmitted signal $g_m(n)\ s(n)$ is unknown and must be estimated by MLE at the mth receive antenna. The LLR at the mth receive antenna branch is calculated using an optimal test within the Neyman-Pearson framework as detailed below:

$$LLR\ (\bar{y}_m) = TS\ (\bar{y}_m) = \ln\left\{\frac{f\bar{w}_m\,(\bar{y}_m;H_1)}{f\bar{w}_m\,(\bar{y}_m;H_0)}\right\}, \tag{11}$$

where $\ln\{\cdot\}$ indicates the natural logarithm, $f\bar{w}_m(\bar{y}_m;H_1)$ and $f\bar{w}_m(\bar{y}_m;H_0)$ are the common joint PDF of $\bar{w}_m$ under H_1 and H_0, respectively. Therefore, LLR test statistic in (11) can be represented as

$$TS\ (\bar{y}_m) = \ln\left\{\frac{f\bar{w}_m\,(\bar{y}_m - \hat{g}_m\,\hat{\bar{s}})}{f\bar{w}_m\,(\bar{y}_m)}\right\} = \sum_{n=1}^{N} \ln\left\{\frac{f\bar{w}_m\,(\bar{y}_m(n) - \hat{g}_m(n)\,\hat{\bar{s}}(n))}{f\bar{w}_m\,(\bar{y}_m(n))}\right\}, \tag{12}$$

where $\hat{g}_m(n)\hat{\bar{s}}(n)$ indicates the vector of MLEs of $g_m(n)s(n)$.

In Cauchy noise environment (α=1), equation (6) can be utilized to substitute the denominator and numerator in (12) with $f\bar{w}_m\,(z) = \dfrac{\gamma_m}{2\pi(|z|^2 + \gamma_m^2)^{\frac{3}{2}}}$, where γ_m indicates the dispersion parameter at mth receive antenna branch. The resulting test statistic $LLR\ (Caushy)$, based on the MLE of $\hat{g}_m(n)\hat{\bar{s}}(n)$ as $y_m(n)$, can be stated as

$$TS_{ch}(\bar{y}_m) = \sum_{n=1}^{N} \ln\left(1 + \frac{|y_m(n)|^2}{\gamma_m^2}\right) \tag{13}$$

Similarly, in Gaussian noise environment (α=2), equation (7) can be utilized to substitute the denominator and numerator in (13) with $f\bar{w}_m\,(z) = \dfrac{1}{2\pi\sigma_m^2}\exp\left(-\dfrac{|z|^2}{2\sigma_m^2}\right)$, where $2\gamma_m = \sigma_m^2$ represents the noise variance at mth receive antenna branch. The resulting test statistic $LLR\ (Guassian)$, based on the MLE of $\hat{g}_m(n)\hat{\bar{s}}(n)$ as $y_m(n)$, can be expressed as

$$TS_{gu}\ (\bar{y}_m) = \frac{1}{2\sigma_m^2}\sum_{n=1}^{N} |y_m(n)|^2 \tag{14}$$

Consequently, the generated output $LLR\ (Y)$ test statistic of the $GLRT$ detector for the specified set $\{|x|_{[i]}\}_{l=1}^{P}$ of the P smallest ranking absolute values observations in the two different noise environments can be expressed as follows:

- Cauchy noise environment (α=1)

$$TS_{APO-ch}(Y) = \sum_{l=1}^{P} \ln\left(1 + \frac{|x|_{[l]}^2}{\gamma_l^2}\right), \tag{15}$$

where γ_l links to the receive antenna dispersion parameter associated with $|x|_{[l]}$.

- Gaussian noise environment (α=2)

$$TS_{APO-gu}(Y) = \sum_{l=1}^{P} \frac{|x|_{[l]}^2}{2\sigma_l^2}, \qquad (16)$$

where σ_l^2 links to the receive antenna noise variance associated with $|x|_{[l]}$. Incidentally, it's worth mentioning that equation (16) is renowned in the field as the energy detector. Thus, the APO scheme introduces $TS_{APO-ch}(Y)$ and $TS_{APO-gu}(Y)$ test statistics, which are deliberately constructed based on the smallest P observations. This design choice is made to mitigate the influence of impulsive noise on the test statistics and enhance their robustness in the presence of such noise disturbances. Following the preceding analysis, the APO spectrum sensing scheme is presented as exposed in Algorithm 1.

Algorithm 1: The APO spectrum sensing under impulsive noise environments

---

1: Compute the sample received observed signal matrix Y

2: Transform matrix Y into one row vector $\bar{x} = \text{vec}(Y)$ of $Y's$ absolute values

3: Sort absolute values of $\bar{x}$ in ascending order

4: Retrieve a specific set P comprising the smallest values from the sorted vector ($\bar{x}$) such as

$\{|x|_{[1]}, |x|_{[2]}, \cdots, |x|_{[P]}\}$

5: // Calculate the test statistic $TS(Y)$ using the retrieved specific set $\{|x|_{[i]}\}_{l=1}^{P}$ and based on the values in α

6: **if** $(\alpha = 1)$ **then**   // Cauchy noise environment

7: Calculate the test statistic $TS(Y) = TS_{APO-ch}(Y)$ in (16)

8: **else**   // Gaussian noise environment $(\alpha = 2)$

9: Calculate the test statistic $TS(Y) = TS_{APO-gu}(Y)$ in (17)

10: **end if**

11: Test if ($TS(Y) > \tau$), then, signal exists (''yes'' decision); otherwise, the signal does not exist (''no'' decision), where the threshold τ is selected to attain a specified level of false-alarm probability.

12: **end**

---

4. Performance Evaluation

Discussions and simulation analysis findings are included in this section, with a particular emphasis on how different system parameters and impulsive noise conditions affect detection performance.

4.1. Simulation Results

The simulation results are discussed in terms of performance metrics, specifically the Receiver Operating Characteristic (ROC) curve. These curves have been generated through a Monte Carlo simulations, with a minimum of 15,000 runs. It's worth noting that the IEEE 802.22 standard's maximum permissible probability of false alarm (P_{fa}) for WRAN (Wireless Regional Area Network) situations is specified at 0.1. In table 1, the simulation parameters are listed.

Table 1: Simulation parameters

Parameter	Value
Number of receive antenna branches (M)	4
Number of primary transmitters (PU)	1
Number of samples collected by a CR (N)	8, 40, 120
α	1, 1.6, 2
γ	1
Number of picking observations (P)	$int(0.1NM), int(0.2NM), \cdots, int(0.9NM),$
P_{fa}	0.1

In the simulation setup, a slowly varying Rayleigh fading channel is considered. This means that the complex channel gains g_m associated with the mth receive antenna, where $E(|g_m|^2) = 1$, may undergo changes at the start of each symbol time. It is assumed, for the sake of simplicity, that total transmit signal power $SP = \sum_{n=1}^{N} |s(n)|^2$ remains constant. This assumption is derived from the normalization of all transmitted signals, where $s(1) = s(2) = \cdots = s(N)$ with $s_Q(n) = s_I(n)$. In the case of the $BIS\ \alpha S$ PDF as described in equation (4), a closed-form expression is not available (with the exception of $\alpha = 1$ and $\alpha = 2$).

Consequently, in this study, the detection threshold has been determined experimentally rather than through theoretical derivation. Therefore, the LLR test statistics have been calculated through numerical simulations using equation (15) for α values of 2, 1.6, and 1, and using equation (16) when α equals 2. The APO scheme will be denoted by the notations APO$_{ch}$ and APO$_{gu}$, with the respective test statistics derived from equations (13) and (14). Moreover, APO$_{gu}$ is exclusively employed in complex Gaussian noise environments due to the established knowledge that the energy detector exhibits significant performance degradation in circumstances with impulsive noise.

4.1.1. Simulation Scenario 1

In this scenario, an assessment is conducted to analyze and investigate the performance of the proposed scheme across different system parameters and requirements. Fig. 2 depicts the ROCs of both the APO_{ch} and APO_{gu} schemes in a BISαS noise environment characterized by $\alpha = 2$ (representing complex Gaussian noise) under various system parameter settings. The sample size N is set to the average value derived from the total number of samples specified in Table 1, while the parameter P varies within the integer range from int($0.4NM$) to NM. As depicted in Fig. 2, it is evident that APO_{ch} in Gaussian noise, specifically when $\alpha = 2$, and APO_{gu} consistently demonstrate superior detection performance across various P values. Furthermore, Fig. 2 also highlights that both APO_{ch} and APO_{gu} exhibit nearly identical performance trends. Therefore, the $ROCs$ of APO_{ch} will be exclusively analyzed in diverse noise environments characterized by Rayleigh fading.
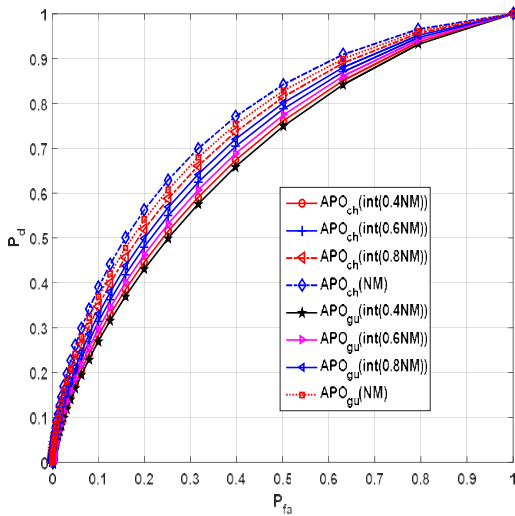
Fig. 2 The $ROCs$ of the proposed APO schemes in complex Gaussian noise environment
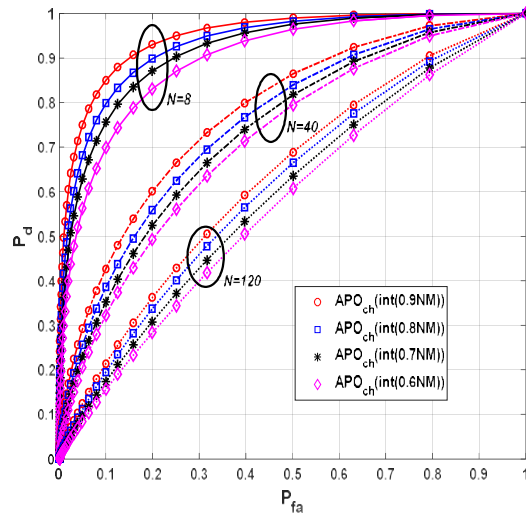
Fig. 3 The $ROCs$ of APO_{ch} within a $BIS\,\alpha S$ noise environment characterized by $\alpha = 2$, across varying values of P and N

Figs. 3 through 5 depict the detection performance of APO_{ch} across a range of N and P values within various noise impulsiveness levels. It is essential to note that when N assumes smaller values, the signal power SP / N per observation is relatively higher. This characteristic results from our choice to maintain a constant total transmit signal power SP. Therefore, when N assumes smaller values, the APO_{ch} detector's performance experiences a significant improvement compared to situations where N is greater. This trend is evident and consistent across all three figures.

In Fig. 3, with the level of impulsiveness held constant in a Gaussian noise environment, it is illustrated that APO_{ch} achieves its highest detection performance when larger values of P are used compared to cases with

smaller P values, regardless of the number of samples N. This observation may be explained by considering that signal components $\{S(n)\}$ traveling through satisfactory channels tend to have higher power, resulting in larger values for the Log-Likelihood Ratio   (LLR).

In Fig. 4, with the level of moderate impulsiveness, i.e., conditions with moderate heavy-tailed noise characteristics, it is demonstrated that APO_{ch} achieves its highest detection performance when a moderate value of P ($int(0.6NM)$) is employed, as compared to other P values, irrespective of the sample size N. This observation can be rationalized by considering that signal components $\{S(n)\}$ affected by favorable channel conditions are treated as a combination of signal and noise, exhibiting moderate power levels. Therefore, in such an environment, opting for a moderate value of P generally yields superior detection performance.
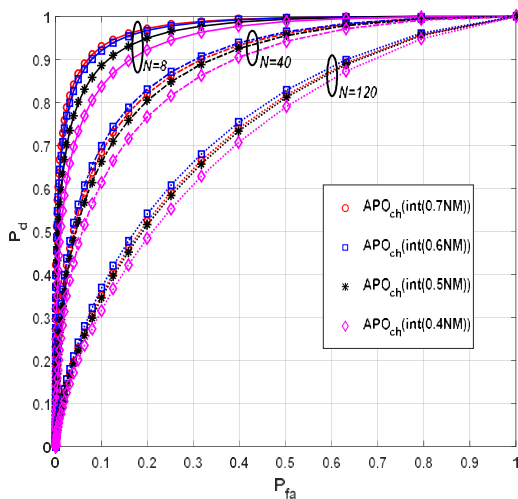
Fig. 4 The $ROCs$ of APO_{ch} within a $BIS\,\alpha S$ noise environment characterized by $\alpha = 1.6$, across varying values of P and N
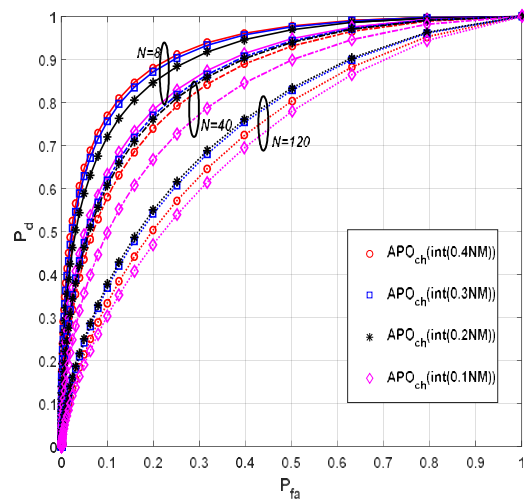
Fig. 5 The $ROCs$ of APO_{ch} within a $BIS\,\alpha S$ noise environment characterized by $\alpha = 1$, across varying values of P and N

In Fig. 5, with severe impulsiveness, i.e., conditions with heavy-tailed noise characteristics, it is revealed that APO_{ch} achieves its highest detection performance when smaller values of P are employed (specifically, $P = int(0.3NM)$), across different numbers of samples N. This finding can be readily explained in the perspective of signal detection. It is widely accepted that an exceptionally large magnitude observation in an impulsive environment should be treated as primarily noise rather than a combination of noise and signal. Consequently, in impulsive environments, a high LLR value is more likely to be associated with noise components as opposed to signal components. Therefore, within such circumstances, opting for a smaller P typically results in superior performance compared to selecting a larger P. Taking inspiration from the observed improvement in detection performance associated with specific P values in particular BISαS noise conditions, the focus will be on detectors configured with $P = int(0.9NM)$ for $\alpha = 2$,

$P = \text{int}(0.6NM)$ for $\alpha = 1.6$, and $P = \text{int}(0.3NM)$ for $\alpha = 1$ within the respective BISαS noise environments in the next simulation scenario.

4.1.2. Simulation Scenario 2

In this scenario, an assessment is carried out to evaluate the superior performance of the proposed APO scheme in comparison to other schemes within the same literature context. The APO scheme is subjected to a comparison with the COS_{EED} spectrum sensing scheme proposed in [18]. The COS_{EED} scheme involves utilizing the enhanced energy detector (*EED*) in each antenna branch and leveraging the combining with order statistics (COS [10]) technique for the detection process. In COS_{EED} scheme, the log likelihood ratio $TS(\bar{y}_m)$ acquired from the *EED* detector in the mth receiving antenna branch can be represented as equation (14) under Gaussian noise conditions. After obtaining M $LLRs$ from the *EED* detectors, an ordering procedure is applied to generate the ordering statistics outlined below:

$$TS_{[\cdot]}(Y) = \{TS_{[1]}(\bar{y}), TS_{[2]}(\bar{y}), \cdots, TS_{[M]}(\bar{y})\}, \qquad (17)$$

where $TS_{[i]}(Y)$ represents the *ith* ordering statistic within $TS(Y)$. Subsequently, K ordering statistics are combined linearly with equal weighting to yield the following test statistic for spectrum sensing:

$$TS_{COS_{EED}}(j_1, j_2, \cdots, j_K; Y) = \sum_{k=1}^{K} TS_{[j_k]}(Y), \qquad (18)$$

where $1 \le j_1 \le j_2 \le \cdots \le j_K \le M$, and K represents the quantity of antenna branches utilized during combining process. In this study, the notation $COS_{EED}(j_1, j_2, \cdots, j_K)$ is utilized to indicate the detector relying on the test statistic in (18). The sample size N is set to the average value derived from the total number of samples specified in Table 1. Fig. 6 demonstrates that the APO$_{ch}$, $COS_{EED}(j_1, j_2)$ and $COS_{EED}(j_1)$ schemes consistently achieve superior detection performance, with APO$_{ch}$ and $COS_{EED}(j_1, j_2)$ schemes sharing the highest detection performance values.

Fig. 7 illustrates that $COS_{EED}(j_1, j_2)$ and $COS_{EED}(j_1)$ schemes experience a moderate decline in performance, whereas APO$_{ch}$ demonstrates a substantial performance improvement. Fig. 8 reveals that the $COS_{EED}(j_1, j_2)$ and $COS_{EED}(j_1)$ schemes experience a substantial decline in performance when operating in very impulsive noise environments, rendering them virtually ineffective as the noise impulsiveness increases. In contrast, APO$_{ch}$ consistently delivers a substantial performance improvement, up to 65% at $P_{fa} = 0.1$, over these schemes within severe impulsive noise environments.

85
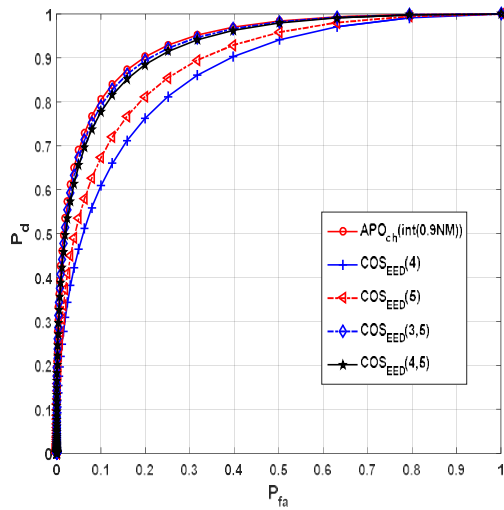
Fig. 6 The $ROCs$ of APO$_{ch}$, $COS_{EED}(j_1, j_2)$, and $COS_{EED}(j_1)$ within a $BIS\,\alpha S$ noise environment characterized by $\alpha = 2$
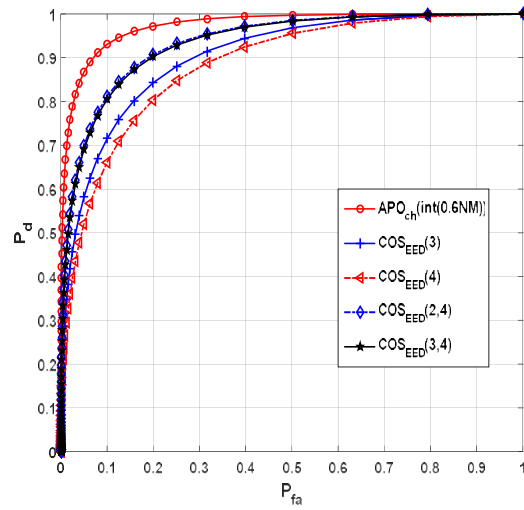
Fig. 7 The $ROCs$ of APO$_{ch}$, $COS_{EED}(j_1, j_2)$, and $COS_{EED}(j_1)$ within a $BIS\,\alpha S$ noise environment characterized by $\alpha = 1.6$
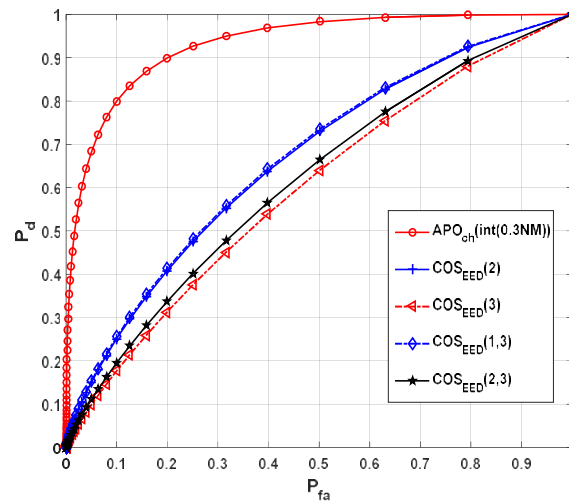
Fig. 8 The $ROCs$ of APO$_{ch}$, $COS_{EED}(j_1, j_2)$ and $COS_{EED}(j_1)$ within a $BIS\alpha S$ noise environment characterized by $\alpha = 1$

The primary distinction between APO and COS_{EED} lies in their methods for deriving the test statistic from the observed data values. In COS_{EED}, the test statistic is formed by linearly combining the K smallest $LLRs$ chosen from a total of M $LLRs$. These $LLRs$ are initially computed individually for every antenna based on N observations. Conversely, in APO, the first step involves selecting the P smallest observations from a total of NM observations collected from M antennas. Subsequently, the test statistic is constructed

using the LLR calculated for those P smallest observations. As a result, the observational values utilized to generate the test statistic for APO have a lower magnitude compared to those employed for COS_{EED}. Therefore, when the noise exhibits increased impulsiveness, the detection performance of APO is expected to surpass that of COS_{EED}.

5. Conclusion

In this paper, a non-linear spectrum-sensing scheme known as the APO is proposed through incorporating the GLRT detector and employing a non-linear diversity-combining approach. The APO utilizes multiple reception antennas to tackle the challenge of spectrum sensing, especially in impulsive noise environments. In addition, the APO introduces APOch and APOgu detectors to mitigate the influence of impulsive noise. The simulation findings yield the following conclusions:

1) The APO scheme offers robust performance and stability in spectrum sensing, especially in impulsive noise environments.

2) The APO scheme delivers reliable spectrum sensing performance with reduced performance variability under scenarios with heavy-tailed noise characteristics.

3) The LLR test statistic for the APO scheme is derived only from a subset of selected observations characterized by their smaller magnitudes tailored to the noise environment. Thus, in impulsive noise environments, a smaller number of observations is selected only to enhance the effectiveness of the scheme.

4) The APO scheme consistently delivers superior detection performance compared to other scheme within the same literature context, COS_{EED}, especially in impulsive noise environments. Moreover, as the degree of impulsiveness in the noise increases, the disparity between the detection performances of the APO and COS_{EED} scheme becomes more pronounced.

Conflicts of Interest

The authors declare no conflict of interest

References

[1] J. Sharad, Y. K. Ashwani, K. Raj and Y. Vaishali, "Cooperative Spectrum Sensing in Cognitive Radio Networks: A Systematic Review," Recent Advances in Computer Science and Communications, vol. 16, no. 4, pp. 2-32, May 2023.

[2] H. Al-Sudani, A. A. Thabit, and Y. Dalveren, "Cognitive Radio and Its Applications in the New Trend of Communication System: A Review," Proceedings of IEEE International Conference on Engineering Technology and its Applications (IICETA 05), Al-Najaf, Iraq, pp. 419-423, May 2022.

[3] D. A. Guimaraes, "Spectrum sensing: A tutorial," Journal of Communication and Information Systems, vol. 37, no. 1, pp. 10–29, Feb 2022.

[4]   C. Vlădeanu, A. Marţian, and D. C. Popescu, "Spectrum Sensing With Energy Detection in Multiple Alternating Time Slots," IEEE Access, vol. 10, pp. 38565-38574, April 2022.

[5]   B. Talukdar, D. Kumar, S. Hoque, and W. Arif, "Estimation based cyclostationary detection for energy harvesting cooperative cognitive radio network," Telecommunications Systems, vol. 79, no. 1, pp. 133-150, Jan 2022.

[6]   S. I. Ojo, Z. K. Adeyemo, and F. K. Ojo, "Energy-efficient cooperative spectrum sensing for detection of licensed users in a cognitive radio network using eigenvalue detector," International Journal of Wireless and Mobile Computing, vol. 23, no. 2, pp. 123-131, Jan 2022.

[7]   J. Manco, I. Dayoub, A. Nafkha, M. Alibakhshikenari, and H. B. Thameur, "Spectrum Sensing Using Software Defined Radio for Cognitive Radio Networks: A Survey," IEEE Access, vol. 10, pp. 131887-131908, Dec 2022.

[8]   A. K. Mandal and S. De, "Analysis of Wireless Communication Over Electromagnetic Impulse Noise Channel," IEEE Transactions on Wireless Communications, vol. 22, no. 2, pp. 1187-1200, Feb. 2023.

[9]   J. Lunden, S. A. Kassam, and V. Koivunen, "Robust Nonparametric Cyclic Correlation-Based Spectrum Sensing for Cognitive Radio," IEEE Transactions on Signal Processing, vol. 58, no. 1, pp. 38-52, Jan 2010.

[10] H. G. Kang, I. Song, S. Yoon, and Y. H. Kim, "A Class of Spectrum-Sensing Schemes for Cognitive Radio Under Impulsive Noise Circumstances: Structure and Performance in Nonfading and Fading Environments," IEEE Transactions on Vehicular Technology, vol. 59, no. 9, pp. 4322-4339, Nov. 2010.

[11] J. Luo, G. Zhang, and C. Yan, "An Energy Detection-Based Spectrum-Sensing Method for Cognitive Radio," Wireless Communications and Mobile Computing, pp. 1-10, 3933336, Feb 2022.

[12] M. B. L. Aquino, J. P. F. Guimarães, A. I. R. Fontes, L. L. S. Linhares, J. B. A. Rego, and A. D. M. Martins, "Circular Correntropy: Definition and Application in Impulsive Noise Environments," IEEE Access, vol. 10, pp. 58777-58786, June 2022.

[13] W. Xu, H. Lai, J. Dai, and Y. Zhou, "Spectrum sensing for cognitive radio based on Kendall's tau in the presence of non-Gaussian impulsive noise," Digital Signal Processing, vol. 123, 103443, April 2022.

[14] A. Halaki, S. Sarkar, S. Gurugopinath, and R. Muralishankar, "Norm-based spectrum sensing for cognitive radios under generalized Gaussian noise," IET Networks, pp. 1–13, June 2023.

[15] C. Zhang, L. Zhang, B. Li, and J. Li, "Similarity measure-based spectrum sensing algorithm under impulsive noise," Wireless Networks, pp. 1-9, June 2023.

[16] M. Liu, N. Zhao, J. Li, and V. C. M. Leung, "Spectrum Sensing Based on Maximum Generalized Correntropy Under Symmetric Alpha Stable Noise," IEEE Transactions on Vehicular Technology, vol. 68, no. 10, pp. 10 262–10 266, Oct 2019.

[17] Z. Luo and E. A. Jonckheere, "Nonlinearity Design With Power-Law Tails for Correlation Detection in Impulsive Noise," IEEE Access, vol. 8, pp. 40667-40679, Mar 2020.

[18] Z. Shabani and A. M. A. Modarres, "A new nonlinear technique for spectrum sensing in the presence of impulsive noise," Proceedings of IEEE Iranian Conference on Electrical Engineering (ICEE 22), Tehran, Iran, pp. 1605-1609, May 2014.